JOURNAL OF THERMOPHYSICS AND HEAT TRANSFER
Vol. 8, No. 2, April–June 1994

Pressure-Based Computational Method for Compressible and Incompressible Flows

S. M. H. Karimian* and G. E. Schneider†
University of Waterloo, Waterloo, Ontario N2L 3G1, Canada

A control-volume-based finite element method with a new formulation for the convecting integration-point velocity for the implicit solution of unsteady compressible and incompressible flows is presented in this article. The method creates a strong coupling between pressure and velocity in incompressible flow on a colocated grid. A pressure-based approach is used to generalize the method for both compressible and incompressible flows. Several quasi-one-dimensional test problems provide validation of the method for Mach numbers ranging from very incompressible flow to supersonic flow with no penalty in accuracy or rate of convergence. Strong shock waves are captured without introducing artificial viscosity.

Nomenclature

A	=	control-volume area
AR	=	area ratio of outlet to throat
C_v	=	specific heat
K	=	conductivity
L	=	distance between "ip" and "up" points
M	=	Mach number
$\dot{m}$	=	mass flow per unit area
P	=	nodal value of pressure
p	=	pressure
S	=	source term
T	=	temperature
t	=	time
U	=	nodal value of velocity
u	=	velocity component
$\hat{u}$	=	convecting velocity
V	=	volume
x	=	Cartesian coordinate
Γ	=	general diffusion coefficient
Δx	=	distance between two nodes
$\Delta\phi$	=	streamwise correction term
δ	=	difference of the neighbor nodal values
Θ	=	dissipation function
μ	=	viscosity
ρ	=	density
ϕ	=	generalized conserved quantity

Subscripts

E, P, W	=	east, center, and west nodal points
e, w	=	east and west integration points
ip	=	integration point
th	=	throat
up	=	upstream point
ϕ	=	related to ϕ

Superscripts

~	=	lagged value from the previous iteration
0	=	lagged value from the old time step

Received May 24, 1993; presented as Paper 93-2768 at the AIAA 28th Thermophysics Conference, Orlando, FL, July 6–9, 1993; revision received Nov. 22, 1993; accepted for publication Nov. 22, 1993.

*Research Assistant, Department of Mechanical Engineering. Member AIAA.
†Professor, Department of Mechanical Engineering. Member AIAA.

Introduction

THE computational methods for solving Navier-Stokes equations are traditionally classified into two categories: 1) methods for compressible flow and 2) methods for incompressible flow.

Some of the methods developed for incompressible flow are based on the stream function-vorticity formulation which has many drawbacks. Primitive variable methods can be easily extended to include three-dimensional flow. The main problem with these methods is the formation of a checkerboard pressure field[1] in incompressible flow. The staggered grid was the first remedy for this problem.[2] With the staggered grid, the components of velocity are not colocated with each other nor with the other problem variables, including pressure. Because of the complications associated with the extension of the staggered grid to two dimensions, the colocated variable methods have strong appeal.

In the Galerkin finite element literature, a number of methods have been proposed for the numerical treatment of transport problems.[3–5] There are also a number of streamline upwind/Petrov-Galerkin (SUPG) methods for fluid flow problems. SUPG methods were originally developed for the incompressible Navier-Stokes equations and have been extended to compressible Euler and Navier-Stokes equations.[6] In control-volume-based finite element methods, the discrete equations are determined by applying conservation balances to defined control volumes. This permits stringent conservation of conserved quantities (e.g., mass, momentum, and energy) throughout the domain and enables physical modeling to be employed in the description of flows crossing the control-volume surfaces. In addition, the finite element basis enables application to complex geometrical domains with ease. These features have been exploited previously by Baliga and Patankar[7] for triangular elements, and by Schneider and Zedan[8] for quadrilateral elements, with extensions by Schneider and Raw[9,10] also for quadrilateral elements.

For compressible fluid flows almost all methods use the continuity equation to solve for density, as a primary variable, and then specify pressure from the equation of state, e.g., Ref. 11. These methods are not efficient for solving incompressible or low Mach number flows. In the incompressible limit numerical difficulties arise in the calculation of pressure from the equation of state, these include 1) roundoff error due to using density as a primary variable,[12] and 2) a time step [or Courant-Freiderichs-Lewy (CFL) number] constraint due to the infinite acoustic speed.[13]

These difficulties can be removed by choosing a pressure-based approach in which pressure is a primary variable and density is found from the equation of state. Van Doormaal

et al.[14] demonstrated that there are no limitations, due to the type of variables, to using a pressure-based method for compressible flow calculations. More recently, pressure-based methods have been used to develop a calculation procedure that is valid for the entire spectrum of Mach numbers.[15-19]

A new formulation for the convecting integration-point velocities, which are used in the continuity equation, is presented in this article. The method creates a strong coupling between pressure and velocity in incompressible flow, and removes any nonphysical oscillations in the solution domain. However, the main contribution of this article is to use the same idea to extend the formulation to compressible flow calculation. The method is fully implicit, and therefore, there is no time step constraint. Several one-dimensional test problems are examined to provide validation of the method for Mach numbers ranging from incompressible flow to supersonic flow.

Computational Formulation

Three significant issues that strongly affect the nature of a computational method are convection-diffusion modeling, colocation of variables in incompressible flow, and compressible flow considerations. Although the results and formulation are presented for one-dimensional flow, the underlying concepts apply equally well for multidimensional flows.

Convection-Diffusion Modeling

Consider the following one-dimensional conservation equation for ϕ, that can stand for velocity or temperature. Note that when $\phi = T$, S_ϕ includes the rest of the terms in the conservation form of the energy equation:

$$\frac{\partial(\rho\phi)}{\partial t} + \frac{\partial(\rho u\phi)}{\partial x} = \frac{\partial}{\partial x}\left(\Gamma\frac{\partial\phi}{\partial x}\right) + S_\phi \tag{1}$$

The one-dimensional grid structure is shown in Fig. 1. After integration over the control-volume, Eq. (1) becomes

$$V\frac{\partial(\widetilde{\rho\phi})}{\partial t} + \sum_{ip}\left[\dot{m}_{ip}\phi_{ip} - \Gamma_{ip}\left(\frac{\partial\phi}{\partial x}\right)_{ip}\right]A_{ip} = \tilde{S}_\phi V \tag{2}$$

where $(\widetilde{\rho\phi})$ and $\tilde{S}_\phi$ are the average values of $(\rho\phi)$ and S_ϕ, respectively, over the control-volume, and the subscript ip is used to denote integration point, as indicated in Fig. 1. When the derivative of a variable is included in the source term, e.g., $\partial P/\partial x$ in the momentum conservation equation, its integral over the control volume would become also a surface integral, e.g., $\Sigma_{ip} p_{ip}A_{ip}$. Nodal values of ρ and ϕ are used to represent $\tilde{\rho}$ and $\tilde{\phi}$, respectively, in the transient term. Since the primary variable is pressure, density is substituted from the equation of state. The diffusion term in Eq. (2) is modeled using a bilinear interpolation of ϕ, which is consistent with the elliptic nature of diffusion. To make the algebraic system of equations well-posed, the integration-point variable for the convection term also needs to be related to nodal variables.

For convection-dominated problems, one would expect that the influence of the upstream value, i.e., ϕ_{up}, would have a large influence on the value of ϕ_{ip}. An appropriate profile assumption for this case would be

$$\phi_{ip} = \phi_{up} + \Delta\phi \tag{3}$$

In one dimension ϕ_{up} would be the upwind nodal value of ϕ. Different approaches have been used to find $\Delta\phi$. One approach is to use Taylor series expansion, whereas a second approach is to evaluate this term based on the physics of the problem. With the second approach an additional equation is needed for each integration-point variable. This equation is obtained by algebraically approximating the nonconservative form of the conservation equation for the variable in question at each integration point. For the generalized conserved quantity this differential equation is given by

$$\rho\frac{\partial\phi}{\partial t} + \rho u\frac{\partial\phi}{\partial x} = \frac{\partial}{\partial x}\left(\Gamma\frac{\partial\phi}{\partial x}\right) + S_\phi \tag{4}$$

For the cases where $\phi = u$ and $\phi = T$, the above equation would be the momentum equation, where $\Gamma = \mu$, and the *thermal* energy equation, where $\Gamma = K/C_v$, respectively. S_ϕ would be different for each case. If the term $\rho u\partial\phi/\partial x$ is modeled by $\rho|u|(\phi_{ip} - \phi_{up})/L$ at the integration point, then ϕ_{ip} can be represented by

$$\phi_{ip} = \phi_{up} + \left\{\frac{L}{\rho|u|}\left[-\rho\frac{\partial\phi}{\partial t} + \frac{\partial}{\partial x}\left(\Gamma\frac{\partial\phi}{\partial x}\right) + S_\phi\right]\right\}_{ip} \tag{5}$$

in which the whole bracket on the right side is the term $\Delta\phi$ [as in Eq. (3)], and is obtained based on the physics of the problem through the rearrangement of Eq. (4) having modeled the convective term as above. All of the terms in $\Delta\phi$ are modeled appropriately.

In the above procedure ϕ_{ip} is obtained only by modeling the convective term in Eq. (4), and the other terms are left to be modeled in the $\Delta\phi$ term. The approach taken by Raw[20] was to approximate all of the terms in the differential equation, i.e., Eq. (4), and then obtain the integration-point variable by rearranging the resulting algebraic equation. With his approach ϕ_{ip} is implicitly affected by all of the terms in the differential equation.

Consider that the flow is from left to right and we are interested in finding the integration-point value of velocity, i.e., $\phi = u$, at the east integration point. The differential equation which should be modeled is the momentum equation, i.e.

$$\rho\frac{\partial u}{\partial t} + \rho u\frac{\partial u}{\partial x} = \frac{\partial}{\partial x}\left(\mu\frac{\partial u}{\partial x}\right) - \frac{\partial p}{\partial x} \tag{6}$$

for which the terms are modeled at the east integration point as follows:

$$\rho u\frac{\partial u}{\partial x} \approx \frac{2\overline{\rho u}}{\Delta x}(u_e - U_P) \tag{7}$$

$$\frac{\partial}{\partial x}\left(\mu\frac{\partial u}{\partial x}\right) \approx 4\mu\frac{(U_E - 2u_e + U_P)}{(\Delta x)^2} \tag{8}$$

$$\frac{\partial p}{\partial x} \approx \frac{(P_E - P_P)}{\Delta x} \tag{9}$$

In order to enhance stability of the method, particularly when a high-pressure gradient is developed in an Euler flow with zero initial velocity, e.g., shock tube problem, the transient term is modeled as

$$\left(\frac{\partial u}{\partial t}\right) \approx \frac{u_e - u_e^0}{\Delta t} + \frac{\tilde{U}_P - U_P}{\Delta t} \tag{10}$$

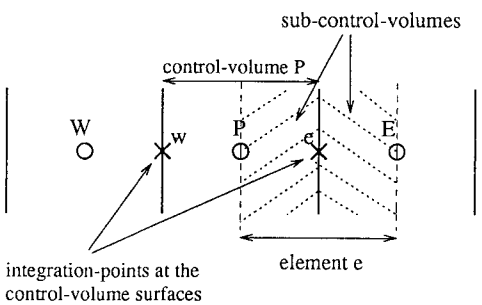

Fig. 1 One-dimensional grid structure.

After substitution of the above approximations in Eq. (6) and rearrangement, the east integration-point velocity for transient viscous flow, that is now connected to the nodal values through the momentum equation, is represented by

$$u_e = \left[\frac{\left(1+\frac{1}{2C}\right)Re+2}{\left(1+\frac{1}{2C}\right)Re+4}\right]U_P + \left[\frac{2}{\left(1+\frac{1}{2C}\right)Re+4}\right]U_E + \left[\frac{\Delta x}{2\overline{\rho u}\left(1+\frac{1}{2C}+\frac{4}{Re}\right)}\right]\left(\frac{P_P-P_E}{\Delta x}\right) + \frac{u_e^0-\tilde{U}_P}{\left(1+2C+\frac{8C}{Re}\right)} \tag{11}$$

where the Courant number is $C = \bar{u}\Delta t/\Delta x$, and the cell Reynolds number is $Re = \overline{\rho u}\Delta x/\mu$. Equation (11) includes all of the physics and relevant couplings for velocity. A similar formulation can be obtained at all integration points. For a steady flow where $C \to \infty$, the integration-point velocity expression becomes

$$u_e = \left(\frac{Re+2}{Re+4}\right)U_P + \left(\frac{2}{Re+4}\right)U_E + \frac{\Delta x}{2\overline{\rho u}[1+(4/Re)]}\left(\frac{P_P-P_E}{\Delta x}\right) \tag{12}$$

Equation (12) can be examined for two limiting cases, i.e., $Re \to 0$ and $Re \to \infty$. For a cell Reynolds number of zero we get

$$u_e = \frac{U_P+U_E}{2} + \frac{(\Delta x)^2}{8\mu}\left(\frac{P_P-P_E}{\Delta x}\right) \tag{13}$$

and for a cell Reynolds number of infinity we get

$$u_e = U_P + \frac{\Delta x}{2\overline{\rho u}}\left(\frac{P_P-P_E}{\Delta x}\right) \tag{14}$$

For a small Reynolds number (approaching zero) the integration-point velocity depends equally on both nodal velocities. As the Reynolds number increases, then so does the influence of the upwind velocity.

The same procedure is applied to the thermal energy equation to obtain the integration-point value of temperature. After approximation, substitution, and rearrangement T_e is obtained as

$$T_e = \left[\frac{\left(1+\frac{1}{2C}\right)Pe+2}{\left(1+\frac{1}{2C}\right)Pe+4}\right]T_P + \left[\frac{2}{\left(1+\frac{1}{2C}\right)Pe+4}\right]T_E + \left[\frac{\Delta x}{2C_v\overline{\rho u}\left(1+\frac{1}{2C}+\frac{4}{Pe}\right)}\right]\left(p_e\frac{U_P-U_E}{\Delta x}+\mu\Theta\right) + \frac{T_e^0-\tilde{T}_P}{\left(1+2C+\frac{8C}{Pe}\right)} \tag{15}$$

where the Peclet number is $Pe = \overline{\rho u}C_v\Delta x/K$, p_e is $(P_E + P_P)/2$, and Θ is the dissipation function. Both u_e and T_e are the integration-point variables that will be used in the convection term of the momentum and energy conservation equations [i.e., Eq. (2) in general], respectively. Since these quantities are convected with the mass flow through the control-volume surface, we call them convected variables. In the next section, modeling of the integration-point velocity that is used in the mass conservation equation will be discussed. This velocity is called the convecting velocity and is denoted with the hat, e.g., $\hat{u}_e$.

Colocation in Incompressible Flow

The problem of pressure-field decoupling, known as the "pressure checkerboard problem," when incompressible flow is modeled on a colocated grid is well known.[1] This problem can be demonstrated by considering the steady one-dimensional Euler flow for which the mass and momentum conservation equations for the control volume P are written as

$$(\rho\hat{u}_e) - (\rho\hat{u}_w) = 0 \tag{16}$$

$$\rho\bar{u}(u_e - u_w) + (p_e - p_w) = 0 \tag{17}$$

If all of the integration-point quantities are substituted using an average of nodal values, then Eqs. (16 and 17) becomes

$$\rho\left(\frac{U_E-U_W}{2}\right) = 0 \tag{18}$$

$$\rho\bar{u}\left(\frac{U_E-U_W}{2}\right) + \left(\frac{P_E-P_W}{2}\right) = 0 \tag{19}$$

With these equations, only the alternate nodal velocities and pressures are connected to each other through the mass and momentum equations, not the adjacent ones. As a result, adjacent pressures and velocities are completely decoupled from each other, and therefore, a checkerboard pressure field can be formed. The main reason for this problem is that the integration-point velocities are not connected to the nodal values based on the physics of the problem. For viscous flows the problem is more subtle, but the pressure decoupling persists. Several approaches to this problem can be found in the literature[18,20,22]; however, it is hard to understand the reason for using specific terms in these methods. Raw[20] proposed to use the same formulation, as obtained for the convected velocity, i.e., Eq. (11), for the convecting velocity in the mass conservation equation to remove the pressure checkerboard problem. A detailed analysis of the method of Ref. 20 and more test problems reveal that this method cannot solve the so-called pressure checkerboard problem when Euler flow is modeled.[21,23]

In this section we will present a method that prevents the formation of a checkerboard pressure field throughout the solution domain. In order to give a clear understanding of the present scheme, the procedure development is briefly outlined.

Consider the convected velocity for the steady incompressible Euler flow, i.e., Eq. (14). This equation is equivalent to the following form:

$$u_e = \frac{U_P+U_E}{2} - \frac{\Delta x}{2\rho\bar{u}}\left(\rho\bar{u}\frac{\delta u}{\delta x}+\frac{\delta p}{\delta x}\right)_e \tag{20}$$

where $\delta u/\delta x$ and $\delta p/\delta x$ are central difference approximations for du/dx and dp/dx, respectively. This means that the integration-point velocity is equal to the average of two nodal values of velocity plus an additional term that includes a form of the momentum equation between two adjacent nodes, i.e.,

P and E. After substitution of u_e from Eq. (20), and u_w from a similar equation into Eq. (17), this equation is rewritten as

$$\rho\bar{u}\left(\frac{U_E - U_W}{2}\right) + \left(\frac{P_E - P_W}{2}\right) = \frac{\Delta x}{2}\left[\left(\rho\bar{u}\frac{\delta u}{\delta x} + \frac{\delta p}{\delta x}\right)_e - \left(\rho\bar{u}\frac{\delta u}{\delta x} + \frac{\delta p}{\delta x}\right)_w\right] \quad (21)$$

In the following analysis, the role of Eq. (20) in a checkerboard field will be shown. By checkerboard field we mean checkerboard pressure or velocity field. If the momentum equation, for a control volume at P, is satisfied using central difference approximations, then the left side of Eq. (21) will be zero. However, such a situation, as is well known,[1] will still permit a checkerboard field. Now, as noted above, the left side of Eq. (21) will be zero for such a field, and therefore, if Eq. (20) is used, resulting in Eq. (21), then the two terms in the parentheses of Eq. (21), i.e., on the right side, will be equal to each other, because the right side is a difference of terms. In fact, the parentheses represent, individually, the momentum equation errors between P and E, and between W and P, respectively, i.e.

$$\varepsilon_e = \left(\rho\bar{u}\frac{U_E - U_P}{\Delta x} + \frac{P_E - P_P}{\Delta x}\right) \quad (22)$$

$$\varepsilon_w = \left(\rho\bar{u}\frac{U_P - U_W}{\Delta x} + \frac{P_P - P_W}{\Delta x}\right) \quad (23)$$

It is noted that the left side of Eq. (21) is identically equal to, in this formulation, the sum of ε_e and ε_w times $\Delta x/2$. This is somewhat fortuitous since, using Eq. (20) for u_e and similarly for u_w in Eq. (17), results in the right side of Eq. (21) being the difference between ε_e and ε_w times $\Delta x/2$. Since, for the checkerboard field, the left side is zero, both ε_e and ε_w must themselves be identically zero, for this case. Thus, with the momentum equation approximations satisfied at P as well as between nodes, there can persist a checkerboard pressure and velocity field. In fact, the only case that does persist is where both velocity and pressure are checkered. This situation is a result of not constraining the integration-point velocity through conservation of mass within the element. However, for consideration of only momentum transport, this is not a serious problem; the problem arises when the coupling between mass and momentum is considered and the mass transporting velocities, i.e., the convecting velocities, must be determined.

In order to remedy the latter problem, a new formulation for the convecting velocity is proposed by using the continuity equation to constrain the velocity field in Eq. (20). Therefore

$$\hat{u}_e = \frac{U_P + U_E}{2} - \frac{\Delta x}{2\rho\bar{u}}[(\text{momentum eq. error}) - \bar{u}(\text{mass eq. error})]_e \quad (24)$$

With this convecting velocity, mass conservation equation becomes

$$\rho\frac{U_E - U_W}{2} = -\rho\frac{\Delta x}{2}\left[\left(\frac{\delta u}{\delta x}\right)_e - \left(\frac{\delta u}{\delta x}\right)_w\right] + \frac{\Delta x}{2\bar{u}}\left[\left(\rho\bar{u}\frac{\delta u}{\delta x} + \frac{\delta p}{\delta x}\right)_e - \left(\rho\bar{u}\frac{\delta u}{\delta x} + \frac{\delta p}{\delta x}\right)_w\right] \quad (25)$$

An analysis similar to that applied for the momentum equation can be used here to conclude that if a checkerboard field tends to be formed in the solution domain, then necessarily the mass equation should be satisfied between nodes P and E, and nodes W and P. Therefore, with the proposed convecting velocity, pressure, and velocity of the middle nodes, e.g., P, are constrained by satisfying both mass and momentum equations in the neighbor elements, e.g., e and w. The structure of the mass and momentum conservation equations can be shown by rearrangement of Eqs. (25 and 21) to be

$$\rho\left(\frac{U_E - U_W}{2}\right) = \left(\frac{P_E - 2P_P + P_W}{2\bar{u}}\right) \quad (26)$$

$$\rho\bar{u}(U_P - U_W) + (P_P - P_W) = 0 \quad (27)$$

The elliptic nature of the pressure is exhibited in the mass conservation equation. One may argue why only the mass equation is not used in the bracket of Eq. (24), i.e., $\hat{u}_e = [(U_E + U_P)/2] - (\Delta x/2\rho\bar{u})(\bar{u}\rho\delta u/\delta x)$. It should be mentioned that in this case in which the mass conservation equation becomes

$$U_P - U_W = 0 \quad (28)$$

there is no effect of downstream pressure on the velocity and pressure of node P. This is in contrast with the elliptic nature of incompressible flow. The proposed idea for the convecting velocity can be generalized to the transient viscous flow. Since the procedures of finding convected and convecting velocities are similar, they can both be obtained simultaneously, i.e., saving computational efforts. The convecting velocity of a general case, at the east integration-point for instance, is given by

$$\hat{u}_e = \frac{U_P + U_E}{2} + \left[\frac{\Delta x}{2\overline{\rho u}\left(1 + \frac{1}{2C} + \frac{4}{Re}\right)}\right]\left(\frac{P_P - P_E}{\Delta x}\right) + \frac{u_e^0 - \left(\frac{\tilde{U}_P + \tilde{U}_E}{2}\right)}{\left(1 + 2C + \frac{8C}{Re}\right)} + \text{TERMS} \quad (29)$$

where

$$\text{TERMS} = \frac{1}{2\overline{\rho u}\left(1 + \frac{1}{2C} + \frac{4}{Re}\right)} \times \left[\bar{u}^2(\rho_E - \rho_P) + \frac{\bar{u}^2}{C}(\rho_e - \rho_e^0)\right] \quad (30)$$

is evaluated using lagged values from the previous iteration. A similar formulation can be written for the west integration point. It is seen that the convecting velocity depends equally on both the nodal velocities, independent of the Reynolds number, and the Courant number. This is the effect of using *both* the continuity and momentum equations at the integration-point to find an expression for the convecting velocity. For an incompressible flow TERMS = 0. For a steady-state compressible Euler flow we further have

$$\hat{u}_e = \frac{U_P + U_E}{2} + \frac{\Delta x}{2\overline{\rho_e u_e}}\left(\frac{P_P - P_E}{\Delta x}\right) + \frac{\bar{u}_e}{2\bar{\rho}_e}(\bar{\rho}_E - \bar{\rho}_P) \quad (31)$$

Several one-dimensional test problems were examined in Ref. 23 and it was found that the new formulation prevents the formation of checkerboard pressure field.

In this article Eqs. (11) and (29) are used for the convected and the convecting velocities, respectively (for the east integration point). Since both convected and convecting velocities are introduced at this stage, it is noted that all of the linearized integration-point velocities (indicated with the lower case u and overbar, e.g., $\bar{u}$), are the lagged values of convecting velocities from the previous iteration, i.e., $\bar{u} = \tilde{u}$.

Compressible Flow Considerations

The main contribution of this article is the generalization of this new formulation to a computational method capable of solving one-dimensional flow problems ranging from incompressible flow to supersonic flow.

In the methods for compressible flow, in which the unknown variables are density, velocities, and temperature, the continuity equation is usually treated as a time-marching equation. In the pressure-based methods, however, the attempt is always to keep the continuity equation as a constraint equation for pressure, which reflects a correct Mach number dependent behavior for pressure. In this regard two issues should be addressed: 1) linearization of the continuity equation and 2) a decision about the value of density at the control-volume face, i.e., integration point.

For a linearization of the mass conservation equation to be appropriate for both subsonic and supersonic flows, both the velocity and density must be allowed to play an active role. The following type of linearization was proposed by Van Doormaal[24]:

$$\rho\hat{u} = \tilde{\rho}\hat{u} + \rho\bar{u} - \tilde{\rho}\bar{u} \tag{32}$$

This linearization of mass flow, which is algebraically equivalent to a Newton-Raphson linearization with respect to both velocity and density, is able to capture changes of both velocity and density in each iteration. Equation (32) permits a smooth transition from incompressible flow, where ρ is nearly constant, to very supersonic flow, where u is nearly constant. Using Eq. (32), Eq. (16) is rewritten as

$$(\tilde{\rho}_e\hat{u}_e - \tilde{\rho}_w\hat{u}_w) + (\rho_e\bar{u}_e - \rho_w\bar{u}_w) = (\tilde{\rho}_e\bar{u}_e - \tilde{\rho}_w\bar{u}_w) \tag{33}$$

In order to close Eq. (33), integration-point densities should be related to the nodal variables. In highly compressible flow the continuity equation acts as a transport equation for density. In this case, evaluation of density at the integration-point should be something similar to that of convected quantities. Therefore, for the east integration-point when flow is from left to right

$$\rho_e = \rho_P + (\overline{\Delta\rho})_e \tag{34}$$

where

$$\overline{\Delta\rho} = -\left[\frac{\Delta x}{2\hat{u}}\left(\frac{\partial\rho}{\partial t} + \rho\frac{\partial u}{\partial x}\right)\right] \tag{35}$$

is evaluated using lagged values from the previous iteration at the integration point, and ρ_P is substituted from the equation of state, e.g., perfect gas

$$\rho_P = (P_P/RT_P) \tag{36}$$

The idea of upwinded density has also been used for solving the transonic full-potential equations.[25,26] As the effect of compressibility becomes more important, particularly in supersonic flow, a smooth transition from elliptic to hyperbolic behavior is exhibited by the continuity equation. To present this property of the algorithm it will be simpler to limit the discussion to steady Euler flow. After substitution of ρ_e and $\hat{u}_e$ from Eq. (34) and Eq. (31), and ρ_w and $\hat{u}_w$ from similar equations into Eq. (33), the conservation form of the steady-state continuity equation for the control volume P is written as

$$\left\{\tilde{\rho}_e\left(\frac{U_P + U_E}{2}\right) + \frac{\bar{u}_e}{2}(\tilde{\rho}_E - \tilde{\rho}_P) + \frac{1}{2\bar{u}_e}(P_P - P_E) - \tilde{\rho}_w\left(\frac{U_W + U_P}{2}\right) - \frac{\bar{u}_w}{2}(\tilde{\rho}_P - \tilde{\rho}_W) - \frac{1}{2\bar{u}_w}(P_W - P_P)\right\} + \left\{\left(\frac{(M_R^2)_e}{\bar{u}_e^2}P_P + \overline{\Delta\rho_e}\right)\bar{u}_e - \left(\frac{(M_R^2)_w}{\bar{u}_w^2}P_W - \overline{\Delta\rho_w}\right)\bar{u}_w\right\} = \{\tilde{\rho}_e\bar{u}_e - \tilde{\rho}_w\bar{u}_w\} \tag{37}$$

where M_R is a reference Mach number whose square is equal to $\bar{u}^2/(RT_{up})$.

In the incompressible flow limit, where $\rho \approx \tilde{\rho}$, the first brace, i.e., $\{\ \}$, is dominant, and the effect of the second brace would be cancelled with the right side. Since difference of densities goes to zero in the limit, Eq. (37) approaches the incompressible formulation of the continuity equation presented by Eq. (26) for which there is no difficulty in convergence. As the result of the pressure/velocity coupling, that was made through the convecting velocity, the continuity equation exhibits the elliptic behavior of flow in this regime.

In the compressible supersonic flow limit, where $\hat{u} \approx \bar{u}$, the effect of the first brace is cancelled with the right side and the second brace becomes more dominant. In this case, the influence of upstream pressures as a function of Mach number increases, and therefore, the hyperbolic nature of the flow is recovered.

It is expected that in the incompressible flow region, i.e., very low Mach numbers, $\Delta\rho$ is represented by the difference of nodal densities, e.g. $(\Delta\rho)_e = (\rho_E - \rho_P)/2$. Therefore, instead of only using Eq. (34) to represent density in Eq. (32), a more accurate approach would be to have a smooth transition of ρ_e from the upstream profile in compressible flow, i.e., Eq. (34), to linear profile in incompressible flow. Mach number should be the governing parameter for this purpose. This can be achieved by introducing

$$\rho_e = \rho_P + (\tilde{\Delta}\rho)_e \tag{38}$$

where

$$(\tilde{\Delta}\rho)_e = \alpha(\overline{\Delta\rho})_e + (1 - \alpha)[(\tilde{\rho}_E - \tilde{\rho}_P)/2] \tag{39}$$

for the east integration point, and a similar equation for the west integration point can be written. Upwind density is substituted by perfect gas equation. The parameter α should be a function of local Mach number. Following the practice of Ref. 27 the following form of α is employed in this study

$$\alpha = [M^2/(1 + M^2)] \tag{40}$$

where $\alpha = 1$ when $M \to \infty$, and $\alpha = 0$ when $M \to 0$. The aforementioned linearization of the continuity equation is more appropriate when the unknown variables are pressure, velocities, and temperature. In the case where the momentum component, i.e., ρu, is the unknown variable, difficulties arise. When density appears explicitly in the continuity equation, it was shown that it can be treated in a way that results in the correct Mach number dependent behavior for pressure. If density and velocity are both included in one unknown variable then it would not be simple to exhibit the dual role of pressure (through the velocity and density) in compressible flow. This will not cause a major difficulty in compressible subsonic flow. However, more theoretical efforts are needed to achieve a set of equations, particularly the mass conser-

vation equation, which correctly exhibits the hyperbolic nature of partial differential equations in supersonic flow.

In order to examine the performance of the new formulation in the compressible flow regime, and with respect to shock location in particular, the proposed method is used to solve a *quasi*-one-dimensional compressible Euler flow. The unknown variables are pressure, temperature, and velocity.

Finite Element Procedure

Following the standard finite element methods, the solution domain is broken up into a number of finite elements with nodes located at every element corner. Within each element there would be a sub-control-volume (SCV) corresponding to each node, as shown in Fig. 1. For each node a control volume is formed by the sub-control-volumes surrounding that node. Although in a control-volume-based finite element method, conservation balance of a conserved quantity holds for every control volume, its formation will be affected by an element-by-element assembly of elemental contributions. For each conservation equation, this elemental contribution is determined by evaluating the source and transient terms over the SCV and the convective and diffusive fluxes at the SCV surface, i.e., integration point. Therefore, at the element level, there would be two SCV equations for each unknown. The assembly procedure will entail the addition of these SCV contributions to the respective control-volume nodal equation.

In the previous sections the integration-point variables, which are used to determine the mass and convective fluxes at the element level, were thoroughly discussed. It is our contention that the modeling of the integration-point quantities is the heart of the computational method development in a control-volume-based approach. More details about the assembly procedure of the control-volume-based finite element methods can be found in Ref. 28.

A few comments about the method should be made. First, the primary goal of the present study is to break the computational barrier between the two flow regimes. Although we do not present the computational performance of the method, our experience shows that there is no difficulty in this regard for both regimes. Second, the present method is second-order accurate in both limits of Euler flow and Stokes flow, and its accuracy falls between first- and second-order when both viscous and inertia forces become important. Third, there is nothing intrinsic about the extension of the method to multidimensional flows. Two-dimensional flow test problems are being computed on unstructured grids.

Numerical Results

Four test problems are examined by the method and good agreement with the exact solution has been achieved. A symmetric converging-diverging nozzle with $AR = 2.035$ is the geometry of the solution domain. The quasi-one-dimensional Euler flow of an ideal gas is solved; note that the numerical formulation presented previously must be modified to include the effects of the variable cross-sectional area for these cases. In all of the results, pressure and temperature are nondimensionalized by the outlet pressure and the inlet temperature, respectively. The duct axis is nondimensionalized by the height of the throat and the grid spacing is uniform in all test problems. Boundary conditions are temperature and mass flow specified in the inlet and pressure specified at the outlet. Since it is the responsibility of the algorithm to calculate the inlet pressure, the accuracy of the code can be checked by the pressure error at the inlet.

In the first case, mass flow and outlet pressure are so designed to achieve a complete subsonic flow in the diverging part of nozzle with sonic flow at throat, i.e., $M_{th} = 1.0$. Fifty-one nodes, i.e., only fifty elements, are used to obtain the results in Fig. 2. Numerical results are indistinguishable from the exact solution (broken line). Sonic flow is achieved with an error in the Mach number of less than 0.5% in the throat.

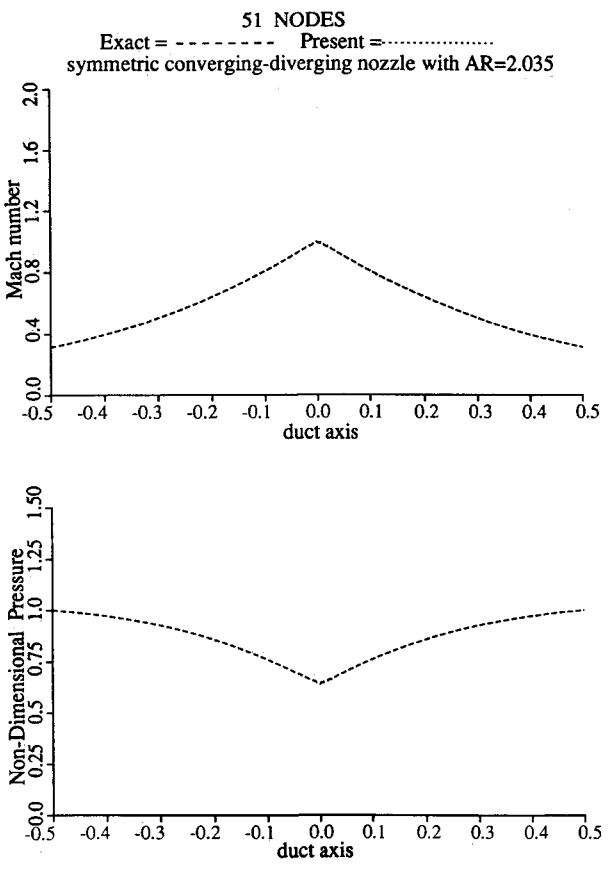

Fig. 2 Converging-diverging nozzle/subsonic flow.

The inlet pressure error, normalized with the inlet dynamic pressure, is within about 0.2%.

When flowfields having a shock wave are numerically solved, oscillations in the vicinity of the shock wave are frequently observed. In order to determine the source of those oscillations related to the continuity and momentum equations, in the second case it is assumed that temperature is constant (isothermal flow), and so the energy equation is not solved. With the same mass flow of the first case, the back pressure is decreased to create a strong shock wave in the diverging part of the nozzle, i.e. $(P_{back}/P_{inlet}) = 0.697$. The Mach number distribution and nondimensionalized pressure distribution are compared with the exact solution in Fig. 3. Numerical results (dotted line) which are obtained on a 75-node grid structure are in excellent agreement with the exact solution. The pressure error at the inlet of this supersonic case is again about 0.2%. This accuracy is achieved by evaluation of ρ_{ip} from Eqs. (38) and (39) in which $\Delta\rho$ is substituted from Eq. (35). More investigation showed that the method of calculation of $\Delta\rho$ highly influences the nature of oscillation around the shock wave. Instead of evaluating $\Delta\rho$ within each element, using nodal values of that element [e.g., nodes E and P for $(\Delta\rho)_e$], $\Delta\rho$ is evaluated at each node using variables of the neighbor nodes [e.g., nodes W and E for $(\Delta\rho)_P$], and then an absolute harmonic interpolation[21] is used to calculate $(\Delta\rho)_{ip}$, i.e., for $(\Delta\rho)_e$

$$(\tilde{\Delta\rho})_e = \frac{|(\tilde{\Delta\rho})_P|(\tilde{\Delta\rho})_E + (\tilde{\Delta\rho})_P|(\tilde{\Delta\rho})_E|}{|(\tilde{\Delta\rho})_P| + |(\tilde{\Delta\rho})_E|} \tag{41}$$

This interpolation favors the term that is smaller in magnitude. The role of the absolutes appears when the two terms do not have the same sign. In this case the interpolation gives a zero value.

If ρ_{ip} is represented by ρ_{up} only, where ρ_{up} is substituted by $P_{up}/(R\tilde{T}_{up})$, then the algorithm would be very robust, but

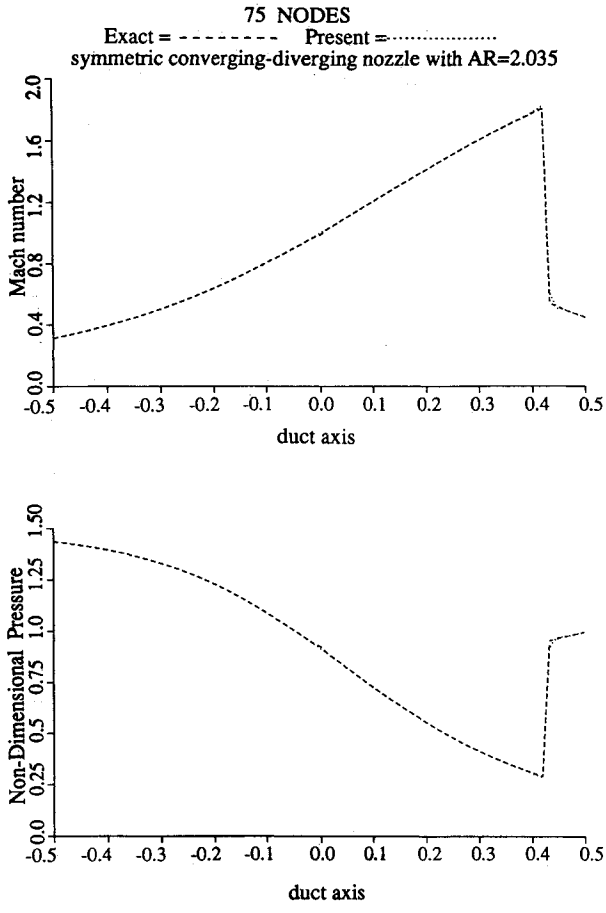

Fig. 3 Converging-diverging nozzle/isothermal flow.

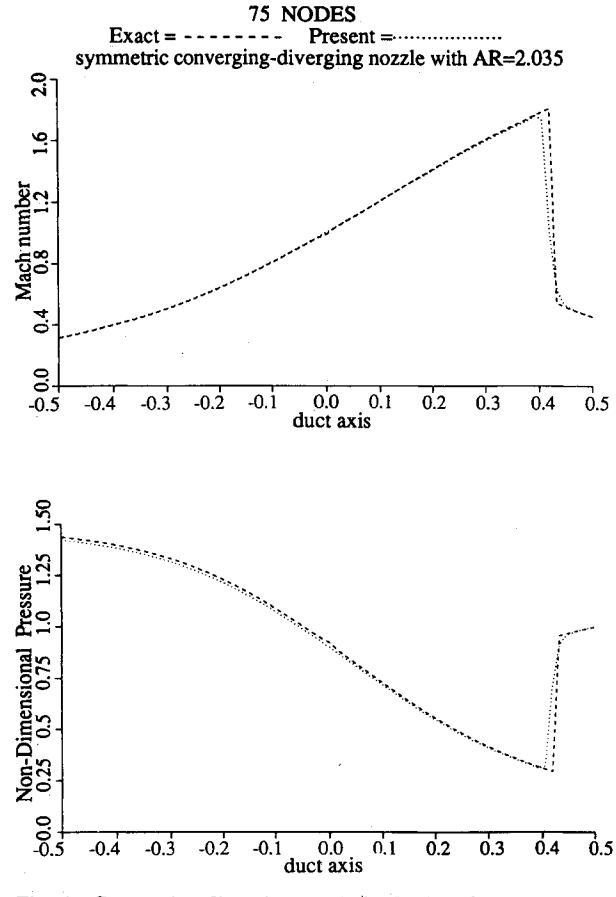

Fig. 4 Converging-diverging nozzle/isothermal flow $\rho_{ip} = \rho_{up}$.

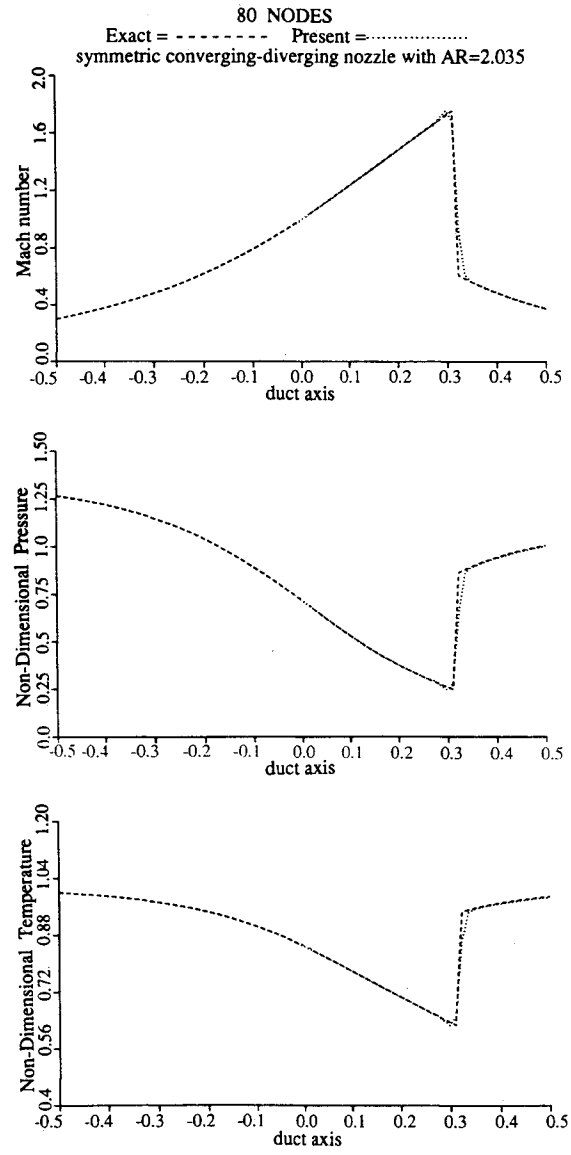

Fig. 5 Converging-diverging nozzle/nonisothermal flow.

accuracy is lost. This is shown in Fig. 4 for which the same problem is solved, but ρ_{ip} is represented by $P_{up}/(R\bar{T}_{up})$. A sharp shock wave is again captured without much effort and demonstrates the robustness. But, as was expected, both numerical diffusion in the vicinity of the shock wave and numerical pressure loss in the whole solution domain with the maximum in the inlet are observed. This is because in this case evaluation of ρ_{ip} is first-order accurate. Excessive dissipation in the vicinity of the shock wave, when a first-order density upwinding is used, has been reported in the literature.[16]

For the fourth case, which is a supersonic ideal gas flow, all of the conditions of the second case remain unchanged, but the number of the nodes is increased to 80. These results correspond to a flow for which the isothermal restriction has been removed. The numerical results are shown in Fig. 5. The accuracy of the temperature and pressure distribution is found to be in excellent agreement with the exact solution. There are very little preshock overshoot and aftershock smearing. For the energy equation, the effect of calculation of T_{ip} on the shock wave is very similar to that of the calculation of ρ_{ip} on the shock wave. Again, $T_{ip} = T_{up}$ increases the robustness of the code, but decreases the accuracy. In short, the difficulty of calculation of T_{ip} across the shock wave was solved in a manner similar to that used for ρ_{ip}. For the Euler flow, where $Pe \to \infty$, $T_e = T_p + (\Delta T)_e$ in which $(\Delta T)_e$

includes the last three terms in Eq. (15), and is computed using absolute harmonic interpolation.

Conclusions

A new control-volume-based finite element formulation for compressible and incompressible fluid flow problems on a colocated grid has been presented. The strong coupling between pressure and velocity through the convecting velocity, and the representation of pressure through density in the continuity equation, have made the algorithm capable of solving a wide range of flow speeds. Since the method approaches the incompressible formulation at very low Mach numbers, i.e., reflecting the elliptic behavior of flow, large time steps will not affect the convergence rate in this regime. The method of calculation of the integration-point density and temperature have resulted in both accurate and oscillation-free solutions for flows with shock waves.

References

[1]Patankar, S. V., *Numerical Heat Transfer and Fluid Flow*, Hemisphere, Washington, DC, 1980, pp. 113–125.

[2]Harlow, F. M., and Welch, J. E., "Numerical Calculation of Time-Dependent Viscous Incompressible Flow of Fluid with Free Surface," *Physics of Fluids*, Vol. 8, No. 12, 1965, pp. 2182–2189.

[3]Donea, J., "A Taylor-Galerkin Method for Convective Transport Problems," *International Journal for Numerical Methods in Engineering*, Vol. 20, No. 1, 1984, pp. 101–119.

[4]Zienkiewicz, O. C., and Taylor, R. L., *The Finite-Element Method*, 4th ed., Vol. 2, McGraw-Hill, New York, 1989, Chaps. 12 and 13.

[5]Pironneau, O., *The Finite-Element Methods for Fluids*, Wiley, New York, 1989, Chap. 4.

[6]Hughes, T. J. R., "Recent Progress in the Development and Understanding of SUPG Methods with Special Reference to the Compressible Euler and Navier-Stokes Equations," *Finite Elements in Fluids*, Vol. 7, Wiley, Toronto, 1987, pp. 273–287.

[7]Baliga, B. R., and Patankar, S. V., "A Control-Volume Finite-Element Method for Two-Dimensional Fluid Flow and Heat Transfer," *Numerical Heat Transfer*, Vol. 6, No. 3, 1983, pp. 245–261.

[8]Schneider, G. E., and Zedan, M., "Control-Volume-Based Finite-Element Formulation of the Heat Conduction Equation," *Spacecraft Thermal Control, Design, and Operation*, edited by P. E. Bauer and H. E. Collicott, Vol. 86, Progress in Astronautics and Aeronautics, AIAA, New York, 1983, pp. 305–326.

[9]Schneider, G. E., and Raw, M. J., "Control-Volume Finite-Element Method for Heat Transfer and Fluid Flow Using Co-Located Variables—1. Computational Procedure," *Numerical Heat Transfer*, Vol. 11, No. 4, 1987, pp. 363–390.

[10]Schneider, G. E., and Raw, M. J., "Control-Volume Finite-Element Method for Heat Transfer and Fluid Flow Using Co-Located Variables—2. Application and Validation," *Numerical Heat Transfer*, Vol. 11, No. 4, 1987, pp. 391–400.

[11]Pulliam, T. H., and Steger, J. L., "Implicit Finite-Difference Simulations of Three-Dimensional Compressible Flow," *AIAA Journal*, Vol. 18, No. 2, 1980, pp. 159–166.

[12]Issa, R. I., "Numerical Methods for Two- and Three-Dimensional Recirculating Flows," *Computational Methods for Turbulence, Transonic and Viscous Flows*, edited by J. A. Essecs, Hemisphere, New York, 1983, pp. 183–211.

[13]Anderson, D. A., Tannehill, J. C., and Pletcher, R. H., *Computational Fluid Mechanics and Heat Transfer*, Hemisphere, New York, 1984, Chaps. 7 and 9.

[14]Van Doormaal, J. P., Raithby, G. D., and McDonald, B. H., "The Segregated Approach to Predicting Viscous Compressible Fluid Flows," *Journal of Turbomachinery, Transactions of the ASME*, Vol. 109, No. 2, 1987, pp. 268–277.

[15]Rhie, C. M., "Pressure-Based Navier-Stokes Solver Using the Multigrid Method," *AIAA Journal*, Vol. 27, No. 8, 1989, pp. 1017, 1018.

[16]Karki, K. C., and Patankar, S. V., "Pressure-Based Calculation Procedure for Viscous Flows at All Speeds in Arbitrary Configurations," *AIAA Journal*, Vol. 27, No. 9, 1989, pp. 1167–1174.

[17]Raw, M. J., Galpin, P. F., and Hutchinson, B. R., "A Co-Located Finite-Volume Method for Solving the Navier-Stokes Equations for Incompressible and Compressible Flows in Turbomachinery: Results and Applications," *Canadian Aeronautics and Space Journal*, Vol. 35, No. 4, 1989, pp. 189–196.

[18]Raw, M. J., Galpin, P. F., and Raithby, G. D., "The Development of an Efficient Turbomachinery CFD Analysis Procedure," AIAA Paper 89-2394, July 1989.

[19]Chen, K. H., and Pletcher, R. H., "Primitive Variable, Strongly Implicit Calculation Procedure for Viscous Flows at All Speeds," *AIAA Journal*, Vol. 29, No. 8, 1991, pp. 1241–1249.

[20]Raw, M. J., "A New Control-Volume-Based Finite-Element Procedure for the Numerical Solution of the Fluid Flow and Scalar Transport Equations," Ph.D. Dissertation, Univ. of Waterloo, Waterloo, Ontario, Canada, 1985.

[21]Stubley, G. D., private communication, Univ. of Waterloo, Waterloo, Ontario, Canada, July 1992.

[22]Rhie, C. M., and Chow, W. L., "Numerical Study of the Turbulent Flow Past an Airfoil with Trailing Edge Separation," *AIAA Journal*, Vol. 21, No. 11, 1983, pp. 1525–1532.

[23]Schneider, G. E., and Karimian, S. M. H., "Advances in Control-Volume Based Finite-Element Methods for Compressible Flows," International Conf. on Computational Engineering Science, Hong Kong, Session B-10, Dec. 1992.

[24]Van Doormaal, J. P., "Numerical Methods for Solution of Compressible and Incompressible Fluid Flows," Ph.D. Dissertation, Univ. of Waterloo, Waterloo, Ontario, Canada, 1985.

[25]Holst, T. L., and Ballhaus, W. F., "Fast, Conservative Schemes for the Full-Potential Equation Applied to Transonic Flows," *AIAA Journal*, Vol. 17, No. 2, 1979, pp. 145–152.

[26]Holst, T. L., "Implicit Algorithm for the Conservative Transonic Full-Potential Equation Using an Arbitrary Mesh," *AIAA Journal*, Vol. 17, No. 10, 1979, pp. 1038–1045.

[27]"Theory Documentation of TASCFLOW Code," Advanced Scientific Computing, Ltd., Waterloo, Ontario, Canada, Version 2.2, Oct. 1992.

[28]Minkowycz, W. J., Sparrow, E. M., Schneider, G. E., and Pletcher, R. H., *Handbook of Numerical Heat Transfer*, Wiley, New York, 1988, pp. 379–421.